RADIATION HARDENED BEAM INSTRUMENTATIONS FOR MULTI-MEGA-WATT BEAM FACILITIES*

K. Yonehara†, Fermilab, Batavia, USA

Abstract

A beam instrumentation is an essential element for the successful operate particle accelerators in which various diagnostics and beam control systems are integrated into beam optics. However, the performance of beam instrumentation is often subject to constraints such as prompt radiation dose, integrated radiation dose, operation (ambient) temperature and humidity, available space, and strength of embedded electromagnetic fields at the monitoring point. These constraints will limit the dynamic range of operational beam parameters, like the maximum achievable beam power. A seamless R&D effort to develop the radiation hardened beam instrumentation should be made for future multi-MW beam facilities. In this paper, we describes about a radiation hardened beam instrumentation based on the operational experience of the NuMI beam line.

INTRODUCTION

A beam instrumentation plays an essential role for ensuring the successful operation of particle accelerators. Its primary function is to characterize a beam phase space by measuring various beam parameters related to an ensemble of charged particles. The beam parameters include:

- Spatial distribution: It determines the spatial characteristics of the charged particle ensemble, which includes the centroid position, orientation, and profile of the beam ensemble.
- Intensity measurement: It involves the amount of beam ensemble in a certain time period.
- Time structure measurement: It includes the time differential beam intensity and the bunch structure of the charged particle ensemble.

There are primarily two beam operational modes in which the beam instrumentation is employed for a distinct purpose. The first mode is the beam commissioning. The beam parameters would be extensively varied to characterize the beam optics. The beam instrumentation should possess sensitivity across a wide dynamics range of the beam parameters. It is often essential to have high sensitivity particularly dealing with low intense beams to measure the tail of the beam distribution. The observed beam parameters are used for determining the Twiss parameter and an aberration, or the extracted beam optics from the measurement is evaluated by comparing to simulation results. During the beam commissioning, a beam operation can often be paused or halted when a beam parameter exceeds a threshold value which would be determined for a machine protection. We should take into account the timing dependence on the beam instrumentation and data with a timing gap in analysis. Once the beam commissioning is done, the accelerator operation transitions into the standard beam operation. The observed beam parameter in the operation mode expects to be stable. A certain level of accuracy on the observed beam parameters is needed to control the accelerator complex and correct the beam parameters by applying a feedback loop system. A concept of feedback loop system differs between a circular accelerator and linear accelerator. Because a beam regulates in an accelerator ring for many revolutions, the beam parameter of the same beam ensemble can be adjusted via a feedback loop system. In contrast, the beam parameter in a linear accelerator cannot be picked up for correcting the beam parameter of the same beam ensemble because the beam passes the accelerator just one time. Therefore, a feedback loop system is applied to correct the beam parameters for the next coming beam ensemble. The beam instrumentation is eventually used as an anomaly detector during the beam operation.

Nowadays major beam facilities have advanced accelerator technology to generate an intense beam for exploring across a wide number of accelerator applications, e.g. a collider, accelerator neutrino beam, intense muon source, spallation neutron source, accelerator driven subcritical nuclear reactor, Radioactive-Isotope (RI) beam, etc. Table1 shows the beam parameter of a selected beam facilities [1,2]. Each facility challenges to develop a radiation hardened beam instrumentation which will be employed in severe environments. Some examples are given in Ref. [1]. In this paper, we address a challenge related to radiation hardened beam instrumentation, especially for a future accelerator neutrino facility based on our experience with the operation of NuMI target system.

ISSUE OF RADIATION DAMAGE ON BEAM INSTRUMENTATION

A radiation dose and integrated energy deposition in a work environment often exceed 10^{10} mSv/hr and 100 MGy, respectively, as reported in Table1. As a result, a material property is drastically changed by radiation. In the NuMI operation, we found that an electrical insulator is lost its high electrical resistivity, a rubber vacuum sealing and vacuum grease are lost a sealing capability, and a semiconductor is lost its electrical property due to a radiation damage. A solid material sometimes exhibits swelling and embrittlement, which can reduce the stress and strain of a component, resulting to loss of its engineering property. We also ob-

* Work supported by ...
† yonehara@fnal.gov

Table 1: Beam parameters reported in the radiation hardened beam instrumentation workshop [3]. A value in a parenthesis is a future plan.

Institution	Beam energy	Beam intensity	Beam power	Radiation dose
CERN CNGS	400 GeV protons	2.4 10^{13} per pulse	500 kW	
CERN LHC	7 TeV protons	1.2 $10^{11} \times 2808$ per beam	362 MJ per beam	
Fermilab NuMI	120 GeV protons	5.5 (6.5) 10^{13} per 1.2 sec	870 kW (1 MW)	10^{10} mSv/hr
Fermilab LBNF	60-120 GeV protons		1.2-2.4 MW	
J-PARC neutrino	30 GeV protons	3.2 10^{14} per 2.48 (1.32) sec	515 (700) kW	
J-PARC MLF	3 GeV protons	4.5 10^{8} per pulse, 25 Hz	730 kW (1 MW)	30 MGy/6y
ESS	2 GeV protons			
SNS	1 (1.3) GeV protons	1.5 10^{14} per beam	1.4 (2) MW	
FRIB	200 MeV/nucleon		400 kW	10^{9} mrem/hr

served that the radiation causes chemical changes of the ambient gas and creates highly reactive chemical species. Those species actively induce rusting a metal, even it is a highly rust resistant metal.

BEAM INSTRUMENTATION IN NUMI

Figure 1 shows the layout of the NuMI target and horn system, including the muon monitors. Every 1.2 seconds, a 120-GeV/c proton beam is transported from the Main Injector to the NuMI target system. The beam spill length is 9.6 μs. The highest beam intensity is 5.6×10^{13} protons on target (POT) per spill demonstrated in Spring 2022. The proton beam structure in the Main Injector and the NuMI proton beam transport line optics are described in [**?**]. The primary beam instrumentation and the muon monitors for the NuMI beam line are described in this section [4].

Proton beam monitor

A pair of induced-charge pickup electrodes and a multi-wire Secondary Emission electron Monitor (SEM) are used as a beam position monitor (BPM) and beam profile monitor (PM), respectively. A special PM, which is permanently placed upstream of the target, is made of a thin (5μmeter thick $\times$ 25 μmeter wide) Ti foil to mitigate the beam scattering at the foil. There are 47×47 foils stretched in x and y directions with gaps between foils of 0.5 mm. The PM provides the proton beam profile for every spill. Other PMs are periodically inserted in the beam line at different locations for monitoring the beam optics. Horizontal and vertical BPMs are paired to measure the beam position on the transverse plane. Two sets of paired BPMs near the target are used for measuring the proton beam position and beam orientation at the target. Several BPMs comprise a network system to automatically correct the proton beam position and beam orientation at the target, which is called the autotune. The accuracy of the beam position measurement is $\pm$0.02 mm using BPM and PM, and the accuracy of the RMS beam spot size measurement is $\pm$0.1 mm using PM.

Current monitor

The proton beam intensity at the target is measured by using a toroidal beam Current Transformer (beam CT) located upstream of the target. The signal calibration is done by using a current source and by comparison to a Direct-Current Current Transformer (DCCT) at the Main Injector. The accuracy of the beam CT is 0.5% while the stability of signal pulse-per-pulse is $\pm$0.1%.

The horn power supply circuit generates a half-sinusoidal voltage, and the pulse is propagated through four striplines. The total pulse length of this half sinusoidal wave is 2.334 msec. A current transformer measures the horn current for each stripline (horn CT). The current transformer is calibrated using a pre-calibrated current source. The accuracy of horn CT is $\pm$0.1%.

Thermocouple beam position sensor

There is a 1.5-mm-diameter Beryllium rod in front of the NuMI target (shown in Figure 2). Two pairs of three Be rods are stretched in transverse plane to intercept the beam. Each pair is directed in horizontal and vertical directions. A gap between rod axial centers is 1.3 mm which corresponds to the expected RMS beam spot size at the target. One end of the rod is attached to a heat sink and other end of the rod is connected to a thermocouple sensor. A proton beam which is delivered into the target deposits its kinetic energy which increases the rod temperature. The thermocouple sensor detects the temperature increment. The thermocouple sensor survives under 10^{10} mSv/hr radioactive environments for several years. The sensor calibration with a known beam intensity needs to be done frequently since the temperature value from the thermocouple sensor is not reliable after the beam irradiation.

Figures 3 and 4 shows the observed beam scan by the thermocouple sensor which was taken in 2018. The beam intensity was fixed around 2.0×10^{13} per beam spill. A solid curve is a Gaussian fit with an offset which is used as a calibration curve. The estimated peak position from the fitting shows the center axis position of the rod and the gap between peaks is the gap of the axis position of the rod. The resolution of horizontal beam scan is worse than the vertical one since ADC of the horizontal thermocouple sensors is coarse.

The beam position at the target is estimated by using the calibration. We use a ratio between the center rod tempera-

Table 2: Table shows the NuMI beam instrumentation and its accuracy. The machine learning can predict those beam parameters.

Beam parameter	Design value	Tolerance	Beam instr.	Accuracy	ML pred.
Horn current	200 kA	±2 kA	Horn CT	0.1%	yes
Horiz. beam position on target	0 mm	±1 mm	BPM, TC	0.02 mm	yes
Vertical beam position on target	0 mm	±1 mm	BPM, TC	0.02 mm	yes
RMS beam spot size	1.3 mm	±0.2 mm	Beam PM	0.1 mm	yes
Beam intensity	50×10^{12} POT	1%	Beam CT	0.5%	yes

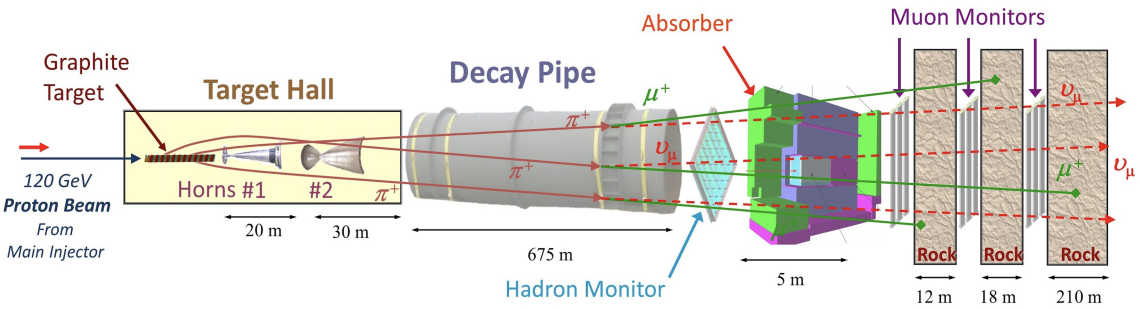

Figure 1: The overall layout of the NuMI beamline.

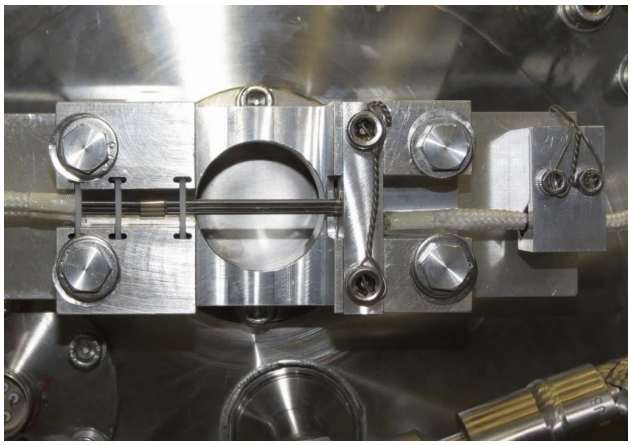

Figure 2: The picture shows the vertical thermocouple sensor.

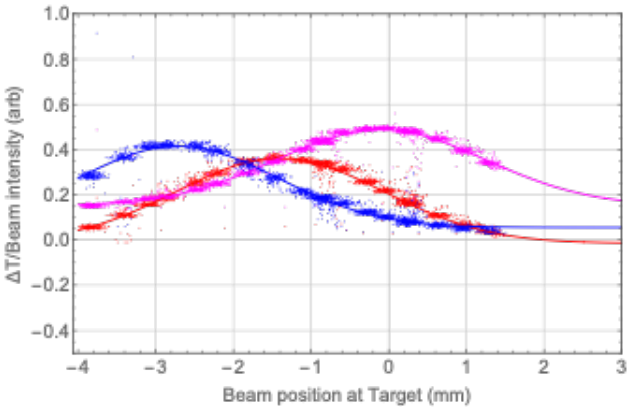

Figure 3: The observed vertical beam scan by using the thermocouple sensor. A red point is the observed temperature at the center rod (f_1), a magenta and blue points are the observed temperate at the top (f_2) and bottom (f_3) rods, respectively.

ture and other two temperature values. Figures 5 and 6 are the estimated vertical and horizontal beam positions at the target from the thermocouple sensor, respectively. A blue solid line is the temperature ratio from the calibration curve. A red point is the target center, a thick red line shows the position range between -0.2 and 0.2 mm, and a thin red line shows the position range between -0.5 and 0.5 mm. A main source of the deviation from the solid line is due to variation of the beam intensity. The thermocouple sensor must be calibrated with the beam intensity.

Other major systematic errors in the thermocouple sensor measurement is a long time constant. Figure 7 shows the observed temperature from one of thermocouple sensors. A blue and orange points are the raw value. Because the NuMI beam time sequence sometimes has a supercycle in which the beam is delivered into the fixed target beam line per every minute. There is a 6 second gap during the supercycle which is sufficiently long to cool the Beryllium rod. The time constant of the thermocouple sensor is roughly a minute so that the temperature observed by the thermocouple sensor never reaches the equilibrium when the supercycle takes place. We chose a data which is close to the equilibrium temperature to estimate the beam position from the thermocouple sensor. Because the thermocouple sensor has several systematic issues, it uses as a backup sensor.

Hadron monitor

The first beam monitor, known as the hadron monitor, is located at the downstream end of the decay pipe. It consists of a 5×5 grid of ionization chamber. Pure helium gas is used as ionization material. The hadron monitor is primarily used for the proton beam-based alignment [4]. The posi-

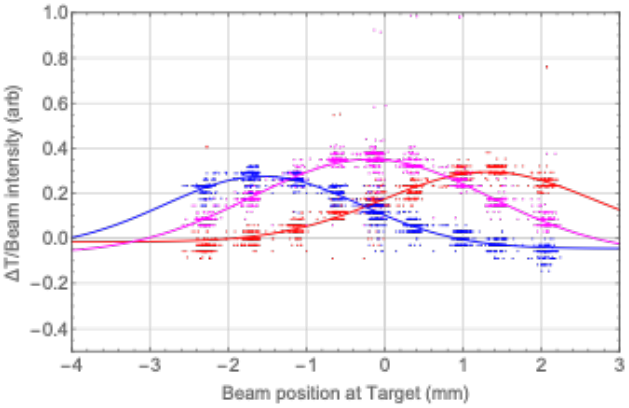

Figure 4: The observed horizontal beam scan by using the thermocouple sensor. A magenta point is the observed temperature at the center rod (g_1), a red and magenta points are the observed temperate at the right (g_2) and left (g_3) rods with respect to the beam direction, respectively.

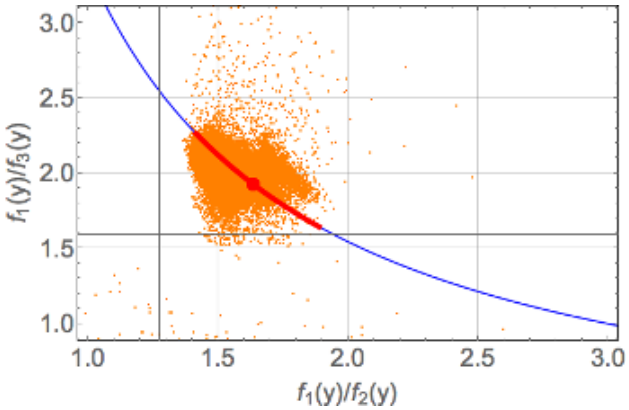

Figure 5: The estimated vertical proton beam position at the target from the thermocouple sensor.

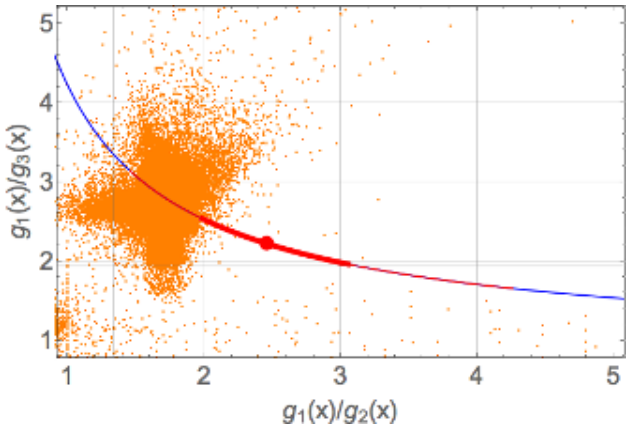

Figure 6: The estimated horizontal proton beam position at the target from the thermocouple sensor.

tions of the target and horns are identified via proton beam tomography. The accuracy of the beam-based alignment is typically ±0.1 mm. It is consistent with the optical survey

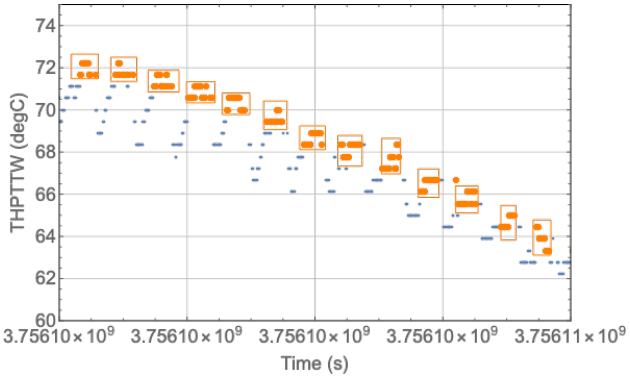

Figure 7: The observed raw temperature value from the thermocouple sensor during the supercycle. An orange box is the analysis gate to select data for estimating the beam position at the target from the theromocouple sensor.

result performed whenever a beam element is installed or replaced in the beamline.

The hadron monitor is directly exposed radiation from the target. The estimated radiation dose at the hadron monitor is $\sim 10^5$ mSv/hr. Because of such a high radiation, the hadron monitor is heavily damaged. Figure 8 shows the hadron monitor which had been operated in the NuMI beam line for a couple of years. The radiation causes chemical changes of the ambient gas and creates highly reactive chemical species. As a result, the surface material of the hadron monitor which is aluminum is rusted.

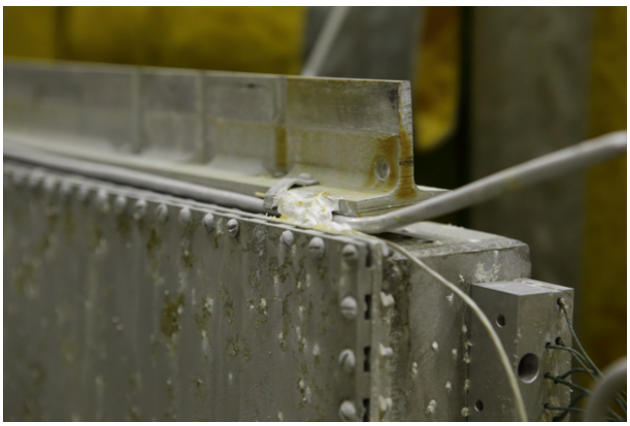

Figure 8: Picture shows the upper right of the hadron monitor which used in the NuMI beamline for a couple of years.

Muon monitors

Figure 9 shows a schematic drawing of the muon monitor. Each muon monitor consists of a 9×9 grid of ionization chambers. Each chamber has a $7.5 \times 7.5\,\mathrm{cm}^2$ sense area Ag-Pt plated electrode on a 1-mm-thick Alumina ceramic electrode base, and the gap between the electrodes is 3 mm. The distance between the centers of channels is 250 mm to cover a $2.1 \times 2.1\,\mathrm{m}^2$ area. Nine ionization chambers are installed in a rectangular aluminum tube. There are nine tubes assembled vertically on a support structure in the beam line.

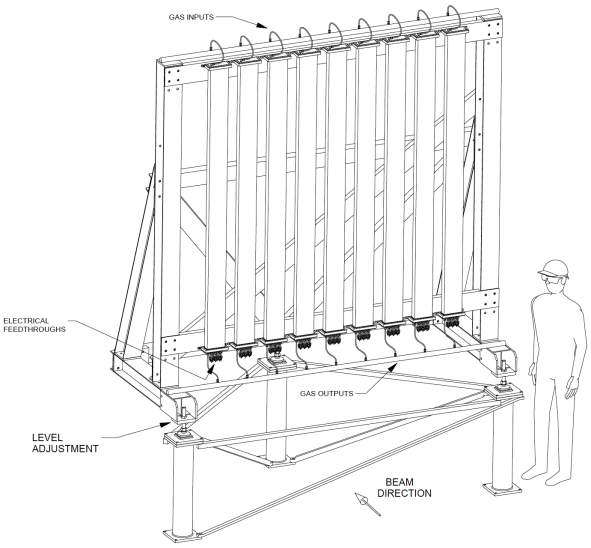

Figure 9: Muon monitor engineering drawing showing the nine tubes containing a row of nine pixels each.

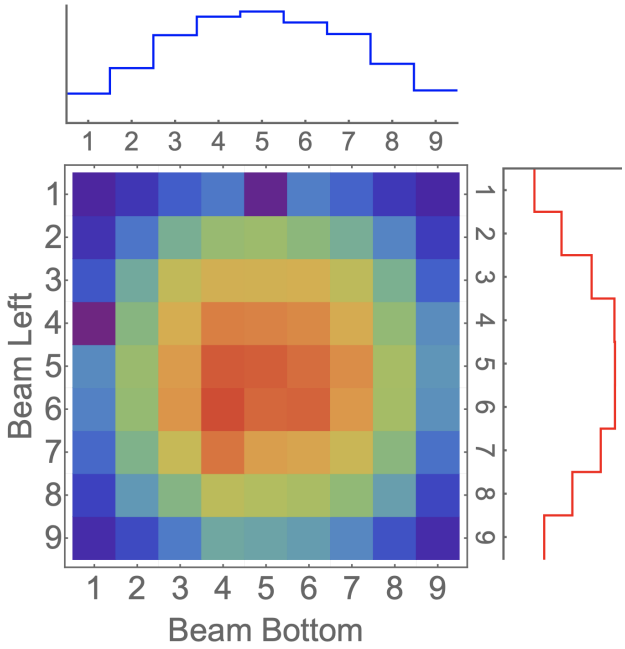

Figure 10: The observed beam profile at Muon Monitor 1. The top and right subplots show the projection of the beam profile in horizontal and vertical planes, respectively. The scale on top and right plots is linear.

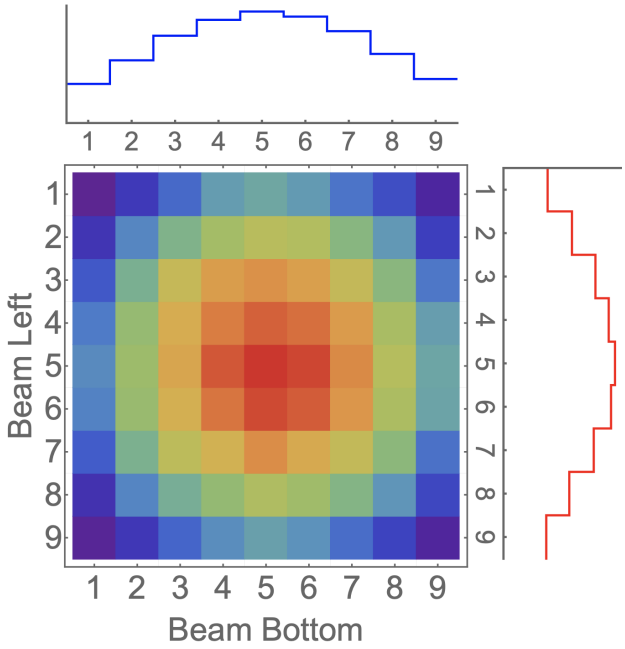

Figure 11: The observed beam profile at Muon Monitor 2. The top and right subplots show the projection of the beam profile in horizontal and vertical planes, respectively. The scale on top and right plots is linear.

Atmospheric-pressure 99.995% pure Helium gas is used as an ionization media, injected from the top and exhausted from the bottom of each tube. The bias voltage is 300 V in which the ionization chamber is on the plateau where all ionized charged particles in the chamber are collected at the electrondes without charge multiplication [4].

Figures 10–12 show an example of the observed pixel image per spill. The pedestal signal, taken when the beam is turned off, is subtracted from the beam-on signal. The size of the pedestal signal is on the order of 0.1% as compared to the beam signal. The signal for each channel was calibrated using a radiation source before the monitor was installed in the beam line. The integrated signal from all channels is normalized by the beam intensity per beam spill and is monitored during beam operation. The long-term fluctuation of the integrated signal normalized by the beam intensity is ±0.2% for Muon Monitors 1 and 2 while the fluctuation of normalized Muon Monitor 3 signal is slightly higher at ±0.5%. It is found that the observed pixel image pattern is not changed by the beam intensity although the signal size is proportional to the beam intensity.

The muon monitors are located downstream of the hadron absorber and separated by 12 and 18 m of rock (see Fig. 1). The muons reaching the monitors lose part of their kinetic energy in the material via energy loss processes. Therefore, the initial spectrum of muons when they are produced differs from the spectrum at the monitors. Figure 13 suggests that each monitor detects a different muon phase space with a specific cutoff energy. It is demonstrated in Sec. **??** that the observed beam profile on the monitors is the result of different horn magnet focusing strengths for different pion energies. Figures **??**–**??** show the simulated phase space of the initial pions for which the daughter muons reach the corresponding muon monitor. Muon Monitor 1 detects the initial pion momentum range above 5 GeV/c, Muon Monitor 2 detects the pion momentum range above 12 GeV/c, and Muon Monitor 3 detects the pion momentum above 25 GeV/c. It should be noted that the observed muon profile on the monitor is a result of the multiple Coulomb scattering

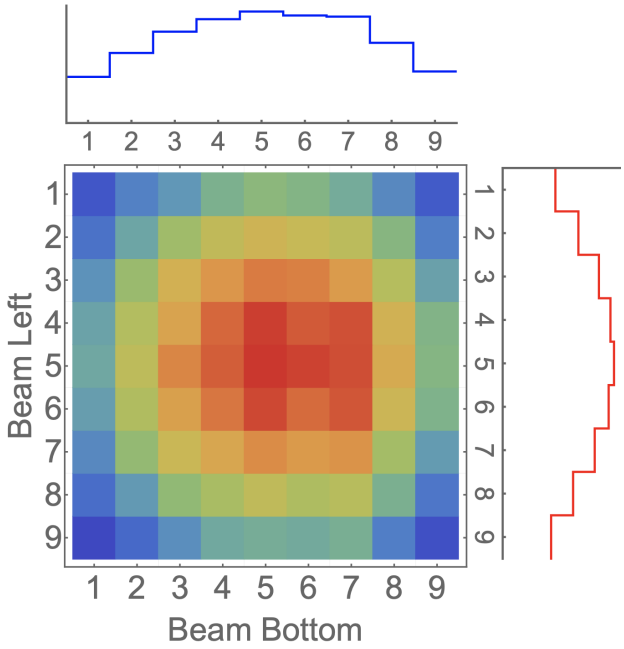

Figure 12: The observed beam profile at Muon Monitor 3. The top and right subplots show the projection of the beam profile in horizontal and vertical planes, respectively. The scale on top and right plots is linear.

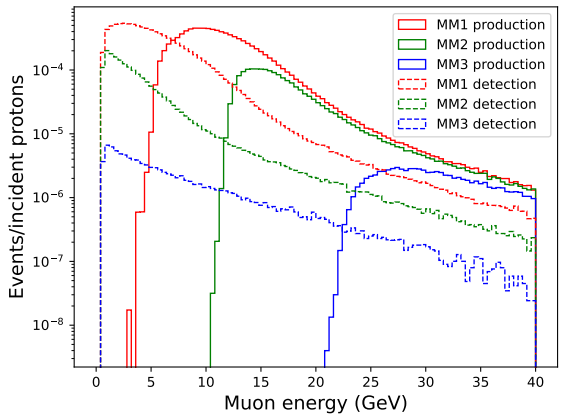

Figure 13: Simulated muon spectra. A solid red line represents the muon spectrum when muons are produced while a dashed red line is the muon spectrum at Muon Monitor 1. The shift is because muons are lost energy in the absorber. The green and blue lines are for Muon Monitor 2 and 3, respectively.

in matter. As a result, muon signals are not correlated with specific neutrino events.

MACHINE LEARNING ALGORITHM TO DETECT BEAM PARAMETERS

The NuMI magnetic horn behave as a linear optics. It suggests that the muon monitor response signal should be linearly related to the beam parameter variations. The muon monitor signal analysis is carried out by using a Machine Learning (ML) algorithm. An advantage of using ML for this application is that it finds correlations among a large number of input parameters and deconvolves them to make a prediction. For example, it is known that the beam intensity affects the horn current because the beam heats the horn conductor by the energy deposition and changes its conductance. By applying ML, the horn current and the beam intensity are detected independently from the observed muon profile.

An Artificial Neural Network (ANN) with multiple hidden layers is used to build the ML architecture. The ANN takes 241 observed values from individual muon monitor channels as inputs. It predicts four beam parameters: horn current, beam intensity, and horizontal and vertical beam positions at the target. Two dead channels on Muon Monitor 1, (row, column) = (1,5) and (4,1) in Fig. 10, are omitted in this analysis. The total number of data points prepared for the study is 13, 563. The data is divided into training (70%) and validation (30%) data to optimize the ANN model architecture. We demonstrated that the ML can predict the critical beam parameters for the NuMI target system operation, which is shown in Table 2.

ACKNOWLEDGEMENTS

We would like to thank the Fermilab Accelerator Operations, Target Systems, External Beam Delivery, and Main Injector Departments for their contributions to this study. We also want to thank the NOvA collaboration for providing us with an opportunity to run the special beam tests.

This work is supported by the Fermi Research Alliance, LLC manages and operates the Fermi National Accelerator Laboratory pursuant to Contract number DE-AC02-07CH11359 with the United States Department of Energy.

This work is partially supported by the U.S. Department of Energy grant DE-SC0019264.

REFERENCES

[1] "Radiation hardened beam instrumentations for multi-MegaWatt beam facilities", K. Yonehara, https://arxiv.org/abs/2203.06024

[2] "High Power Targetry R&D and support for future generation accelerator", F. Pellemoine et al., JINST 18, T07006, 2023, https://iopscience.iop.org/article/10.1088/1748-0221/18/07/T07006

[3] "Radiation Hardened Beam Instrumentation Workshop", https://indico.fnal.gov/event/52543/

[4] "Exploring the Focusing Mechanism of the NuMI Horn Magnets", K. Yonehara et al., https://arxiv.org/abs/2305.08695